Vapor−Liquid Equilibria and Interfacial Tensions of Associating Fluids within a Density Functional Theory

Dong Fu[†] **and Jianzhong Wu***[,‡]

Department of Environmental Engineering, North China Electric Power University, Baoding, P.R. China 071003, and Department of Chemical and Environmental Engineering, University of California, Riverside, California 92521-0425

A self-consistent density functional theory is applied to investigating the phase behavior and interfacial tensions of water and low-molecular-weight normal alkanols. For the bulk phases, the density functional theory is reduced to an equation of state that provides an accurate description of saturation pressures as well as vapor−liquid phase diagrams. Near the critical region, the long-range fluctuations are taken into account using a renormalization group theory. With the same set of molecular parameters, the theory yields satisfactory results for both bulk properties and surface tensions of the associating fluids investigated at all temperatures.

1. Introduction

Interfacial properties of fluids are essential for many industrial applications relating to thin liquid films, emulsions, foams, dispersions, adsorption-based separations, and heterogeneous chemical reactions.[1−4] A variety of conventional models are available for the correlation and occasionally prediction of interfacial properties such as surface and interfacial tensions, adsorption isotherms, capillarity condensation, nucleation and bubble formation, micellization, and so on.[5,6] Although traditional models have played important roles in the applications of surface sciences and will continue to do so in the near future, their limitations become evident when microscopic properties such as the behavior of fluids in micropores or the structures of self-assembled surfactant molecules are of concern. Moreover, many conventional models of interfacial phenomena follow phenomenological approaches that often entail semiempirical parameters that can be obtained only by fitting to the experimental data under direct investigation.

Over the past several decades, statistical mechanics and molecular simulations have been extensively applied to the interpretation of various interfacial behaviors of fluids such as wetting, capillary condensation, and nucleation, and remarkable progress has been achieved.[7,8] There is no doubt that these more modern approaches will become increasingly important for understanding novel interfacial phenomena emerging from various frontiers of surface science. However, it is also fair to state that practical examples of the successful application of these new approaches to the quantitative interpretation of experimental data or the design of industrial processes remain scarce. Molecular modeling of interfacial behavior of realistic systems is often restricted by the use of oversimplified theoretical models or by limitations on computer power.

The most viable approach for modeling the interfacial properties or inhomogeneous behavior of fluids is probably density functional theory (DFT), a formalism of statistical mechanics that emphasizes one-body densities instead of microstates. The mathematical framework of DFT was first established by Hohenberg and Kohn[9] in the context of the quantum many-body theory of electrons, and it was later recognized that the same fundamental theorem is also applicable to classical systems. A comprehensive review of the early literature on classical DFT was given by Evans,[10] and its applications have recently been reviewed by Lowen[11] and by Oxtoby.[12] Although the construction of DFT relies heavily on achievements from more traditional methods, it has a number of advantages in comparison with a variety of more traditional statistical mechanical approaches.

Recently, we have developed a version of DFT for complex fluids that is able to quantitatively account for the effects of various inter- and intramolecular forces on the free energy functional.[13−21] Extensive comparison with results from molecular simulations for a number of model systems shows that the theory is promising for the representation of the the structural and thermodynamic properties of a variety of practical systems including highly asymmetric electrolytes and copolymers in the bulk as well as under confinement. For systems with uniform density profiles, our DFT reduces to a versatile equation of state that is similar to the well-known statistical associated fluid theory (SAFT).[22,23]

The purpose of this work is to test the applicability of the new density functional theory in the correlation/prediction of the bulk and interfacial properties of realistic associating fluids with a single set of molecular parameters. The self-consistency of bulk and interfacial models is important for practical applications because, whereas bulk properties are often readily measurable, the experimental results for interfacial properties are sparse. With molecular parameters obtained from easily accessible bulk properties, a self-consistent molecular theory can be used to predict the properties of a fluid under various confined geometries that are normally inaccessible to simple experiments.

There have been a number of earlier applications of DFT to the modeling of realistic associating fluids. In particular, Chapman and co-workers investigated the structures of four-site water-like molecules in hard slit pores and near functionalized surfaces.[24−26] Good agreement was achieved between theory and simulations. A

* To whom correspondence should be addressed. E-mail: jwu@engr.ucr.edu.
[†] North China Electric Power University.
[‡] University of California, Riverside.

10.1021/ie049788a CCC: $30.25
Published on Web 07/23/2004

similar approach was recently used to investigate the effect of confinement on the chemical equilibrium of associating fluids in slit pores.[27] Sokolowski and coworkers have utilized DFT to study associating fluids between planar walls, vapor−liquid interfaces of dimerizing Lennard-Jones fluids, the effect of confinement on interfacial structures, and the bulk- and confined-phase behaviors of binary mixtures of associating fluids exhibiting closed-loop immiscibility.[28−35] Recently, DFT has also been used to represent the vapor−liquid nucleation of dimerizing fluids and the micellization of amphiphilic molecules.[36,37] Not only does the present work distinguish itself from all previous investigations in the context of density functional theory, but more importantly, it represents the first effort toward modeling both phase behavior and interfacial properties of realistic associating fluids using a single set of molecular parameters.

2. Theoretical Model

2.1. Density Functional Theory. According to the mathematical theorem of Hohenberg and Kohn,[9] the grand potential of an open system, $\Omega[\rho(\mathbf{R})]$, is a unique functional of the equilibrium molecular density distribution, $\rho(\mathbf{R})$, which can be obtained by solving the variational equation

$$\frac{\delta\Omega[\rho(\mathbf{R})]}{\delta\rho(\mathbf{R})} = 0 \tag{1}$$

Here, $\mathbf{R}$ stands for the configuration of a molecule. Once the equilibrium density profile is solved, one can determine both structural and thermodynamic properties of the system from the grand potential functional given *a priori*. The key is how to formulate an accurate grand potential that faithfully represents the nonideality of the system under consideration. This distinguishes various versions of classical density functional theory.

Formally, the grand potential, $\Omega[\rho(\mathbf{R})]$, is related to the Helmholtz energy functional, $F[\rho(\mathbf{R})]$, through the Legendre transform

$$\Omega[\rho(\mathbf{R})] = F[\rho(\mathbf{R})] - \int[\mu - \psi(\mathbf{R})]\rho(\mathbf{R})\,\mathrm{d}\mathbf{R} \tag{2}$$

where $\mathrm{d}\mathbf{R}$ represents integration in configurational space, μ stands for the chemical potential, and $\psi(\mathbf{R})$ is an external potential applied to each molecule. For a free vapor−liquid interface, the external potential is $\psi(\mathbf{R}) = 0$.

The associating fluids considered in this work are represented by normal alkanols and water. We assume that water molecules are spherical particles with four bonding sites standing for the lone electron pairs of the oxygen atom and the two hydrogen atoms of each molecule, and normal alkanols are homogeneous chains with one associating site. The van der Waals attractions between spherical segments are represented by an exponentially decaying function of the center-to-center separation. In the absence of associations and chain connectivity, the intermolecular potential is reduced to the well-known hard-core Yukawa (HCY) model.

The Helmholtz energy functional is given by[13−15,20,38]

$$F[\rho(\mathbf{R})] = F^{\mathrm{id}}[\rho(\mathbf{R})] + F^{\mathrm{hs}}[\rho(\mathbf{R})] + F^{\mathrm{dis}}[\rho(\mathbf{R})] + F^{\mathrm{chain}}[\rho(\mathbf{R})] + F^{\mathrm{assoc}}[\rho(\mathbf{R})] \tag{3}$$

where $F^{\mathrm{id}}[\rho(\mathbf{R})]$ corresponds to the Helmholtz energy functional for an ideal gas with the same molecular density profile, and the superscripts hs, dis, chain, and assoc denote the contributions due to the hard-sphere repulsion, attractive interaction, chain connectivity, and associations, respectively. The Helmholtz energy functional of an ideal gas is exactly known as

$$F^{\mathrm{id}}[\rho(\mathbf{R})] = kT\int \mathrm{d}\mathbf{R}\,\{\rho(\mathbf{R})[\ln[\rho(\mathbf{R})\Lambda^3 - 1]\} \tag{4}$$

where k is the Boltzmann constant, T is absolute temperature, and Λ denotes the thermal wavelength of a molecule. All other terms on the right-hand side of eq 3, designated as the excess Helmholtz energy functional, can be derived only approximately. The excess Helmholtz energy functional is attributed to nonbonded intermolecular interactions. As in our earlier work, we assume that this term depends only on the density distributions of individual segments. In this work, we assume further that all segments are identical and indistinguishable from each other. In this case, the molecular density is related to the segmental density by $\rho(\mathbf{R}) = m\rho(\mathbf{r})$, where m is the number of segments in each molecule.

The Helmholtz energy functional due to the short-ranged repulsion is represented by a modified fundamental measure theory (MFMT) recently proposed by Yu and Wu[16] and independently by Roth et al.[39] This modification preserves all of the advantages of the original FMT of Rosenfeld[40] but provides improved structural and thermodynamic properties of hard-sphere fluids in the bulk and under inhomogeneous conditions. As in the original FMT,[40] MFMT conjectures that the excess intrinsic Helmholtz energy functional can be expressed in the form

$$F^{\mathrm{ref}}[\rho(\mathbf{r})] = kT\int \mathrm{d}\mathbf{r}\,\{f^{\mathrm{hs}}[n_\alpha(\mathbf{r})] + f^{\mathrm{chain}}[n_\alpha(\mathbf{r})] + f^{\mathrm{assoc}}[n_\alpha(\mathbf{r})]\} \tag{5}$$

where the local Helmholtz energy densities $f^{\mathrm{hs}}[n_\alpha(\mathbf{r})]$, $f^{\mathrm{chain}}[n_\alpha(\mathbf{r})]$, and $f^{\mathrm{assoc}}[n_\alpha(\mathbf{r})]$ are functions of six scalar and vector-weighted densities, $n_\alpha(\mathbf{r})$, defined as

$$n_\alpha(\mathbf{r}) = \int \mathrm{d}\mathbf{r}'\,\rho(\mathbf{r}')\,w^{(\alpha)}(\mathbf{r} - \mathbf{r}') \tag{6}$$

The weight functions $w^{(\alpha)}(\mathbf{r})$ with the indices $\alpha = 0$, 1, 2, 3, V_1, and V_2, are linked to the geometry of a single particle of radius R as follows

$$w^{(2)}(\mathbf{r}) = \delta(R - r), \qquad w^{(3)}(\mathbf{r}) = \Theta(R - \mathrm{r}), \qquad w^{(V_2)}(\mathbf{r}) = (\mathbf{r}/r)\delta(R - r) \tag{7}$$

$$n_0(\mathbf{r}) = \frac{n_2(\mathbf{r})}{4\pi R^2}, \qquad n_1(\mathbf{r}) = \frac{n_2(\mathbf{r})}{4\pi R}, \qquad \mathbf{n}_{V_1}(\mathbf{r}) = \frac{\mathbf{n}_{V_2}(\mathbf{r})}{4\pi R} \tag{8}$$

Whereas the local Helmholtz density $f^{\mathrm{hs}}[n_\alpha(\mathbf{r})]$ in the original FMT is formulated in the framework of the scaled-particle theory, MFMT takes advantages of the more accurate Carnahan−Starling equation of state for hard spheres. The local Helmholtz density is divided into scalar (denoted by the superscript S) and vector (denoted by the superscript V) contributions

$$f^{\mathrm{hs}}[n_\alpha(\mathbf{r})] = f^{\mathrm{S}}[n_\alpha(\mathbf{r})] + f^{\mathrm{V}}[n_\alpha(\mathbf{r})] \tag{9}$$

with

$$\frac{f^{S}[n_\alpha]}{m^2} = -n_0 \ln(1-\zeta_3) + \frac{n_1 n_2}{1-\zeta_3} + \left[\frac{\ln(1-\zeta_3)}{36\pi n_3^2} + \frac{1}{36\pi n_3 (1-\zeta_3)^2}\right] n_2^3 \quad (10)$$

$$\frac{f^{V}[n_\alpha]}{m^2} = -\frac{\mathbf{n}_{V_1}\cdot\mathbf{n}_{V_2}}{1-\zeta_3} - \left[\frac{\ln(1-\zeta_3)}{12\pi n_3^2} + \frac{1}{12\pi n_3 (1-\zeta_3)^2}\right] n_2 \mathbf{n}_{V_1}\cdot\mathbf{n}_{V_2} \quad (11)$$

where m is the number of segments in a chainlike molecule and $\zeta_3 = m\pi n_0 \sigma^3/6$ is the packing fraction. The scalar part is identical to that from the Carnahan–Starling equation of state.[41] In the limit of a uniform fluid, the two vector-weighted densities $\mathbf{n}_{V_1}(\mathbf{r})$ and $\mathbf{n}_{V_2}(\mathbf{r})$ as well as the vector Helmholtz energy vanish, and eq 9 becomes identical to the Carnahan–Starling equation.[41]

In our earlier work,[14,15] we also derived the contributions due to chain connectivity and association, respectively, as follows

$$f^{\text{chain}}[n_\alpha] = (1-m)\ln[g^{\text{hs}}(\sigma)] n_0 \zeta \quad (12)$$

where $\zeta = 1 - \mathbf{n}_{V_2}\cdot\mathbf{n}_{V_2}/n_2^2$ and $g^{\text{hs}}(\sigma)$ is expressed as

$$g^{\text{hs}}(\sigma) = \frac{1}{1-\zeta_3} + \frac{3}{2}\frac{\zeta_2 \zeta}{(1-\zeta_3)^2} + \frac{1}{2}\frac{\zeta_2^2 \zeta}{(1-\zeta_3)^3} \quad (13)$$

with $\zeta_2 = m\pi n_0 \sigma^2/6$ and

$$f^{\text{assoc}} = \sum_{\text{A}} n_0 \zeta \left[\left(\ln X^{\text{A}} - \frac{X^{\text{A}}}{2}\right) + \frac{1}{2}\right] \quad (14)$$

where M is the number of association sites on each molecule. In eq 14, $\sum_{\text{A}}$ represents a sum over all associating sites on the molecule, and X^{A} is the mole fraction of molecules not bonded at site A, which is given by

$$X^{\text{A}} = [1 + N_0 \sum_{\text{B}} n_0 \zeta X^{B} \Delta^{\text{AB}}]^{-1} \quad (15)$$

where N_0 is Avogadro's number and Δ^{AB} is

$$\Delta^{\text{AB}} = g^{\text{hs}}(\sigma)[\exp(\epsilon^{\text{AB}}/kT) - 1](\sigma^3 \kappa^{\text{AB}}) \quad (16)$$

where κ^{AB} and ϵ^{AB}/k stand for the volume and energy of association, respectively.

The Helmholtz energy functional due to the van der Waals attractions is given by the quadratic density expansion[38]

$$F^{\text{dis}}[\rho(\mathbf{r})] = m \int d\mathbf{r}\, f_0^{\text{dis}}[\rho(\mathbf{r})] + \frac{kTm^2}{4}\int\int d\mathbf{r}'\, d\mathbf{r}\, c(|\mathbf{r}-\mathbf{r}'|;\bar{\rho})[\rho(\mathbf{r}) - \rho(\mathbf{r}')]^2 \quad (17)$$

where $f_0^{\text{dis}}[\rho(\mathbf{r})]$ is the contribution of dispersion to the Helmholtz energy density for a uniform fluid at the local density $\rho(\mathbf{r})$, and $c(|\mathbf{r}-\mathbf{r}'|;\bar{\rho})$ denotes the attractive part of the direct correlation function at an average density of

$$\bar{\rho} = [\rho(\mathbf{r}) + \rho(\mathbf{r}')]/2 \quad (18)$$

The Helmholtz energy density of bulk hard-core Yukawa fluids, f_0^{dis}, has been derived from the mean-spherical approximations (MSA).[42,43] The equations for f_0^{dis} and the corresponding equation of state are reproduced in Appendix II. The analytical expression for the direct correlation functions of Yukawa fluids was recently reported by Tang.[44]

2.2. Renormalization Group (RG) Theory. For bulk systems, eq 3 reduces to an equation of state that is essentially the same as SAFT. Although the non-mean-field theory is able to account for the short-ranged correlations due to the intermolecular forces, it is inadequate to represent the long-range fluctuations near the critical point of vapor–liquid equilibrium. For that purpose, we employ a renormalization group (RG) theory of classical fluids originally proposed by White[46–50] for the correction of the dispersion contribution to the Helmholtz energy. We assume that the short-ranged repulsion, chain connectivity, and association have negligible effects on the critical fluctuations.

During the renormalization group iteration, a sequence of corrections to the Helmholtz energy density, δf_n, $n = 1, 2, \ldots$, are added to the initial Helmholtz energy density, $f_0(\rho) = f_{\text{s}}[\bar{\rho}_{\text{s}}(\mathbf{r})]$, which ignores the contributions due to the long-wavelength fluctuations. The recursion equation is given by[51]

$$f_n(\rho) = f_{n-1}(\rho) + \delta f_n(\rho) \quad (19)$$

where the differential Helmholtz energy density at each step n, δf_n, is calculated from

$$\delta f_n(\rho) = -K_n \ln \frac{\Omega_n^{\text{s}}}{\Omega_n^{\text{l}}}, \qquad 0 \le \rho < \rho_{\max}/2 \quad (20)$$

with

$$K_n = \frac{1}{\beta V_{\text{D},n}} = \frac{1}{2^{3n}\beta L^3} \quad (21)$$

$$\Omega_n^{\alpha}(\rho) = \int_0^{\rho} dx \exp\left[-\frac{\bar{f}_n^{\alpha}(\rho+x) + \bar{f}_n^{\alpha}(\rho-x) - 2\bar{f}_n^{\alpha}(\rho)}{2K_n}\right], \quad \alpha = \text{s, l} \quad (22)$$

$$\bar{f}_n^{\text{l}}(\rho) = f_{n-1}(\rho) + \alpha m^2 \rho^2 \quad (23)$$

$$\bar{f}_n^{\text{s}}(\rho) = f_{n-1}(\rho) + \alpha m^2 \rho^2 \frac{\psi \bar{\omega}^2}{2^{2n+1}\bar{L}^2}, \qquad \bar{L} = \frac{L}{\sigma} \quad (24)$$

In eqs 20–24, $\rho_{\max}$ is the maximum possible molecule density, and α and $\bar{\omega}^2$ depend on the intermolecular potential $u(r)$

$$\alpha = -\frac{1}{2}\int u(|\mathbf{r}-\mathbf{r}'|)\, d\mathbf{r} = 2\pi\epsilon\frac{1+\lambda}{\lambda^2} \quad (25)$$

Table 1. Regressed Parameters for Nine Associating Fluids[a,b]

	σ (10^{-10} m)	ϵ/k (K)	ϵ^{AB}/k (K)	κ^{AB}	m	T (K)	ARD (%) p	ARD (%) ρ^L
methanol	3.224	201.4	2670.5	0.068	1.475	290−430	2.9	2.9
ethanol	3.370	198.0	2900.0	0.034	1.823	273−443	1.3	2.9
propanol	3.450	210.3	2850.1	0.032	2.201	293−483	2.7	4.0
butanol	3.600	208.4	2750.3	0.070	2.352	390−485	4.5	1.5
pentanol	3.600	210.0	3000.8	0.044	2.785	327−467	2.8	4.2
acetic acid	3.792	246.2	2498.3	0.140	1.420	293−503	1.8	2.9
hydrogen sulfide	3.692	201.4	829.4	0.337	1.009	212−340	1.9	1.4
ammonia	3.172	205.9	1320.1	0.167	1.093	210−370	0.6	0.8
water	2.934	290.1	2858.8	0.023	1.026	283−493	2.7	2.8
ARD (%)							2.3	2.6

[a] Experimental data taken from the literature.[52] [b] Number of association sites $M = 3$ for water and $M = 2$ for all other associating fluids.

and

$$\bar{\omega}^2 = -\frac{1}{3!\alpha\sigma^2}\int r^2 u(|\mathbf{r}-\mathbf{r}'|)\,d\mathbf{r} = \frac{1}{3}\left[\frac{6+6\lambda+3\lambda^2+\lambda^3}{\lambda^2(1+\lambda)}\right] \quad (26)$$

where λ is the range parameter for the Yukawa potential.

In our calculations, there are six adjustable parameters for each chainlike fluid: segment number m, hard-sphere diameter of each segment σ, dispersion energy parameter of each segment ϵ/k, association volume κ^{AB}, association energy ϵ^{AB}/k, and average gradient of the wavelet function ψ. The parameters m, σ, ϵ/k, κ^{AB}, and ϵ^{AB}/k can be obtained by regressing the experimental data[52,53] far from the critical temperature. The parameter ψ is obtained by fitting to the critical temperature and pressure from experiments.[52] L is adopted as 2.0σ according to the work of Jiang and Prausnitz.[49] No additional parameters are introduced to represent the interfacial properties.

3. Results and Discussion

3.1. Vapor−Liquid Phase Diagram. For bulk phase equilibrium calculations, the DFT reduces to an equation of state that is equivalent to SAFT. With the RG correction near the critical point, the Helmholtz energy has no analytical expression. As a result, both the pressure and chemical potential that are required in the vapor−liquid equilibrium calculations must be obtained via numerical methods.

Table 1 presents the regressed parameters and the average relative deviations (ARDs, %) of the liquid-phase density, ρ^L, and saturation vapor pressure, p^V, for nine associating fluids. From Table 1, we find that the theory results in a satisfactory phase diagram, including the critical region. Figures 1−3 present the vapor−liquid coexistence curves and the saturation pressures in comparison with experimental data from the literature.[52] Also shown in these figures are the results from the corresponding equations of state without the RG correlation. As expected, the analytical theories significantly overpredict the critical temperatures. With the RG correlation, the equation of state is able to represent both the bulk phase behavior and the thermodynamic properties accurately. Table 2 presents a comparison between the critical temperature and pressure before and after the RG correction is applied. One can see that the calculated T_c and p_c values are greatly improved by the RG correction. The average relative deviations for T_c and p_c before the RG correction are 3.7% and 31.8%, respectively, whereas after the RG correction, the corresponding values become 0.5% and 2.1%.

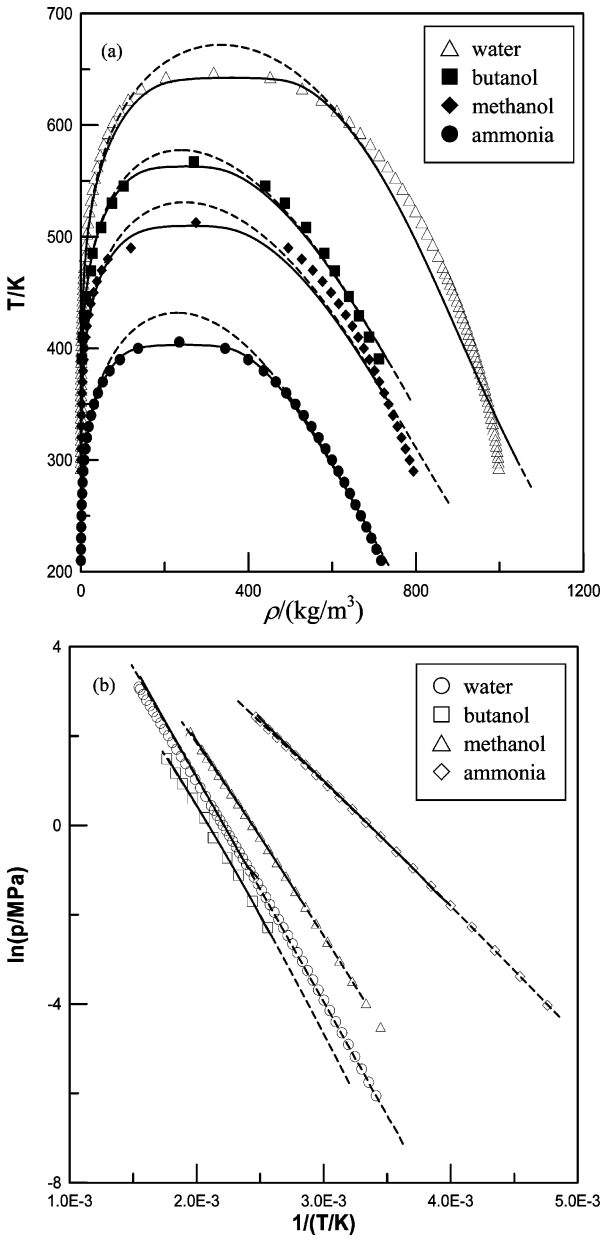

Figure 1. (a) Phase diagrams and (b) saturation pressures of water, methanol, butanol, and ammonia. (Symbols: experimental data.[52] Lines: —, with the RG correction; − − −, without the RG correction.)

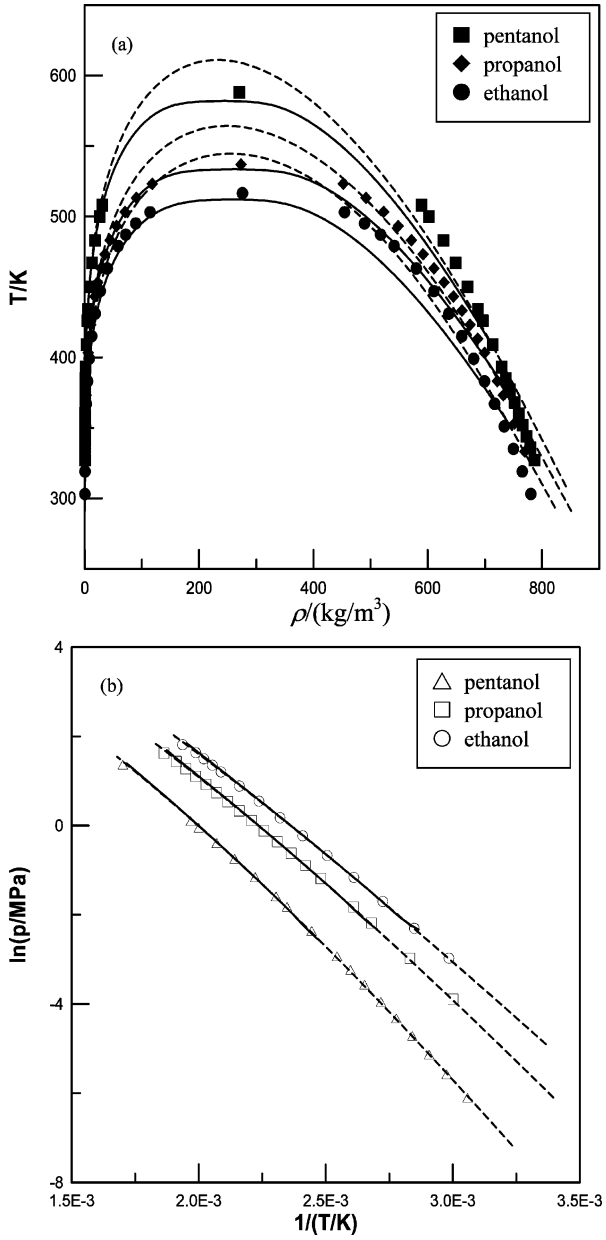

Figure 2. (a) Phase diagrams and (b) saturation pressures of ethanol, propanol, and pentanol (Symbols: experimental data.[52] Lines: —, with the RG correction; – – –, without the RG correction.)

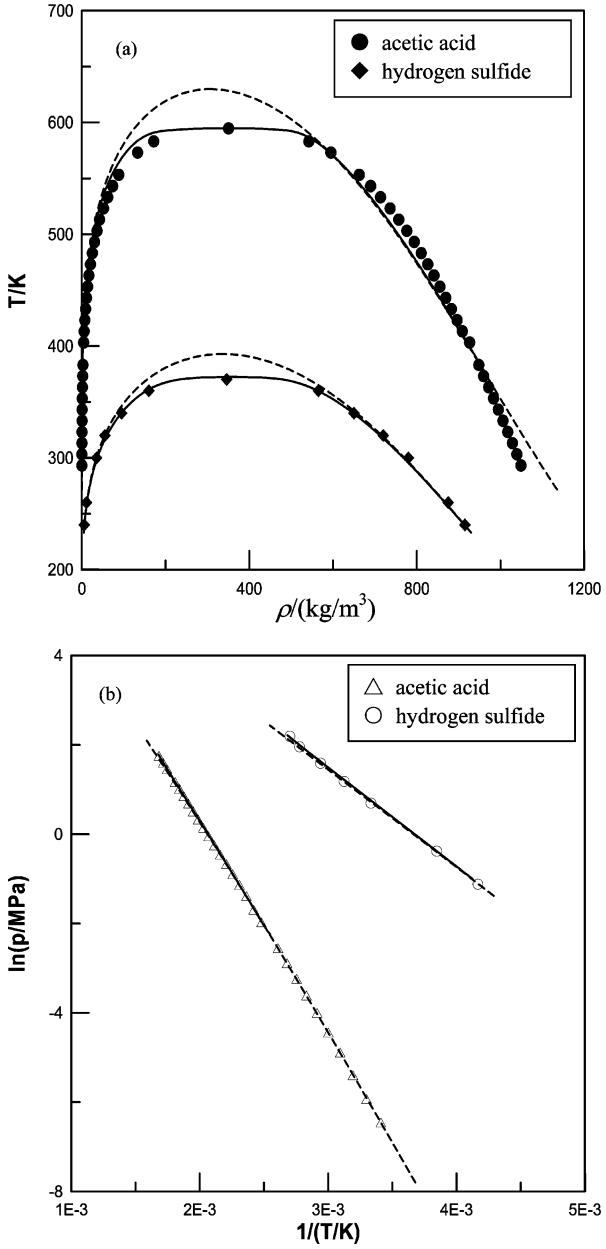

Figure 3. (a) Phase diagrams and (b) saturation pressures of acetic acid and hydrogen sulfide (Symbols: experimental data.[52] Lines: —, with the RG correction; – – –, without the RG correction.)

3.2. Surface Tension. Using the coexisting vapor and liquid densities obtained from the phase diagram calculations as an input, we can calculate the equilibrium density, $\rho(\mathbf{r})$, across the vapor−liquid interface using the DFT. Because the density varies only in the direction perpendicular to the interface (z direction), the Euler−Lagrange equation becomes

$$\left(\frac{\partial f^{\mathrm{id}}[\rho(z)]}{\partial \rho(z)} + \frac{\partial f^{\mathrm{ref}}[\rho(z)]}{\partial \rho(z)} + \frac{\partial f^{\mathrm{dis}}[\rho(z)]}{\partial \rho(z)}\right) - \mu = 0 \quad (27)$$

The detailed expressions for the partial derivatives appeared on the left-hand side of eq 27 are given in Appendix I.

Equation 27 is solved using the standard Picard method. Specifically, the initial guess for the density profile is given by

$$\rho(z) = \begin{cases} \rho^{\mathrm{V}}, & z \le 0 \\ \rho^{\mathrm{L}}, & z > 0 \end{cases} \quad (28)$$

The density $\rho(z)$ is updated using eq 27, and the process is continued until convergence is achieved.

Figure 4 presents the interfacial density profiles for methanol. The density profiles vary smoothly between the bulk densities as predicted by the classical square-gradient theory.

Once the interfacial density profile has been obtained, the surface tension can be calculated from

$$\gamma = \int_{-\infty}^{\infty} [f[\rho(z)] - \rho(z)\mu + p]\, \mathrm{d}z \quad (29)$$

where p stands for pressure. With the equilibrium liquid

Table 2. Comparison between the Calculated T_c and p_c and the Experimental Data

		T_c (K)			p_c (MPa)		
	Ψ	exp	cal[b]	cal[c]	exp	cal[b]	cal[c]
methanol	8.0	512.7	509.8	530.9	8.10	7.96	10.1
ethanol	8.5	516.4	512.1	526.1	6.10	6.32	7.56
propanol	9.0	534.6	533.6	549.9	5.20	5.39	6.57
butanol	10	567.0	563.5	577.6	4.40	4.42	5.2
pentanol	10	588.2	582.5	595.8	3.90	4.00	4.66
acetic acid	8.5	594.8	595.2	629.9	5.90	5.92	8.09
hydrogen sulfide	7.5	373.1	372.6	392.8	8.94	9.16	11.4
ammonia	7.0	405.6	403.4	431.8	11.30	11.70	16.5
water	9.5	647.3	641.6	672.0	22.10	22.3	36.1
ARD (%)			0.5	3.7		2.1	31.8

[a] Experimental data taken from the literature.[52] [b] Results with the RG correction. [c] Results without the RG correction.

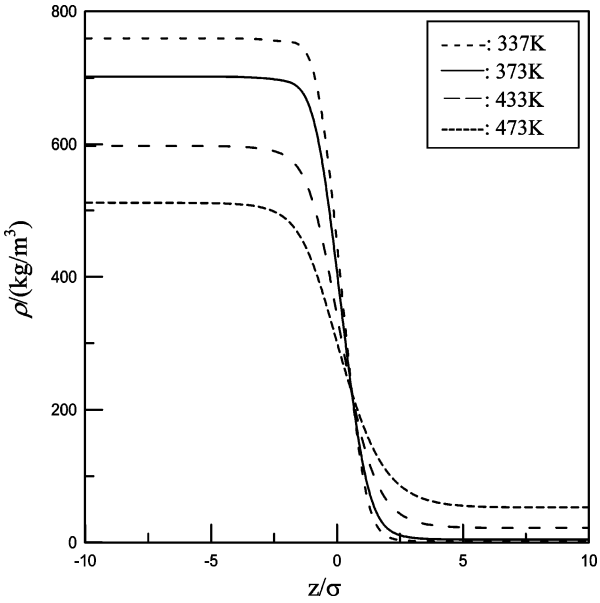

Figure 4. Interfacial density profiles of methanol predicted from the density functional theory.

and vapor densities as the input, the present DFT correctly captures the quantitative features of the dependence of the interfacial tension on temperature and yields satisfactory results for both the phase equilibria and the surface tensions by taking into account both the long-range and short-range correlations. Figures 5−7 compare the surface tensions of nine associating fluids predicted with the current DFT and those from experiments. We find that, for all of the systems investigated in this work, the predictions are quite satisfactory.

We find that multiple sets of molecular parameters could fit the phase equilibrium data equally well. For instance, the molecular parameters for water, $\sigma = 3.13 \times 10^{-10}$ m, $\epsilon/k = 485.4$ K, $\epsilon^{AB}/k = 1156.2$ K, $\kappa^{AB} = 0.051$, and $m = 1$ result in small average relative deviations for the coexisting densities and vapor pressure (0.8% for vapor pressure and 1.2% for liquid density); as shown in Figure 5, however, this set of parameters yields unsatisfactory interfacial tension. Because the main purpose of this work is to demonstrate that both the bulk and interfacial properties can be described using a single set of molecular parameters, the values reported in Table 1 were obtained by fitting to the experimental data for both phase equilibrium and surface tension simultaneously.

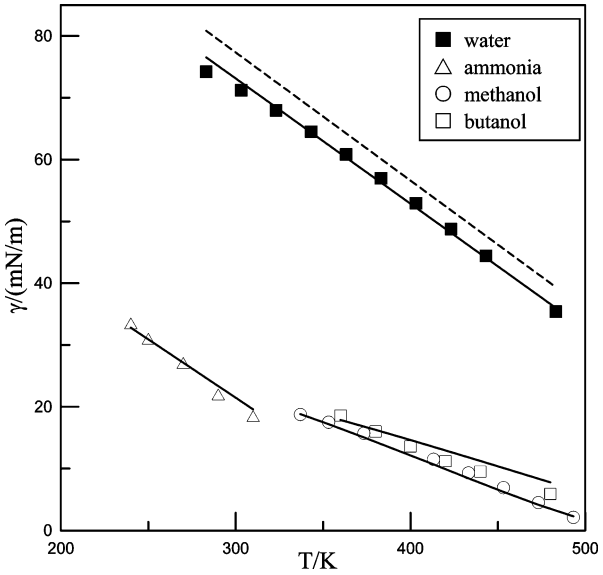

Figure 5. Surface tensions of water, methanol, butanol, and ammonia. (Symbols: experimental data.[52,53] Lines: —, calculated with the MFMT; − − −, surface tensions of water calculated with the MFMT using the parameters $\sigma = 3.13 \times 10^{-10}$ m, $\epsilon/k = 485.4$ K, $\epsilon^{AB}/k = 1156.2$ K, $\kappa^{AB} = 0.051$, and $m = 1$.)

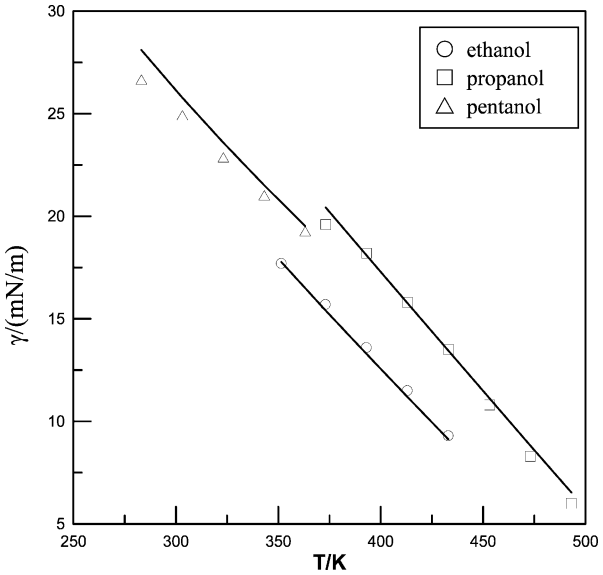

Figure 6. Surface tensions of ethanol, propanol, and pentanol (symbols, experimental data;[52,53] lines, calculated with the MFMT).

4. Conclusions

We have shown that, with the direct correlation functions for the bulk fluids as the input, it is feasible to construct a self-consistent density functional theory that yields accurate bulk phase behavior and interfacial properties using a single set of molecular parameters. The theory is applied to nine associating fluids, and the calculated results for both the phase equilibria and surface tensions are in good agreement with the experimental data. In addition to the phase equilibria and the interfacial properties, the self-consistent thermodynamic framework proposed in this paper can also be applied to model the structure of associating fluids. We leave that for our future work.

Acknowledgment

This work was supported in part by the National Science Foundation (Grant CTS-0340948). D.F. also

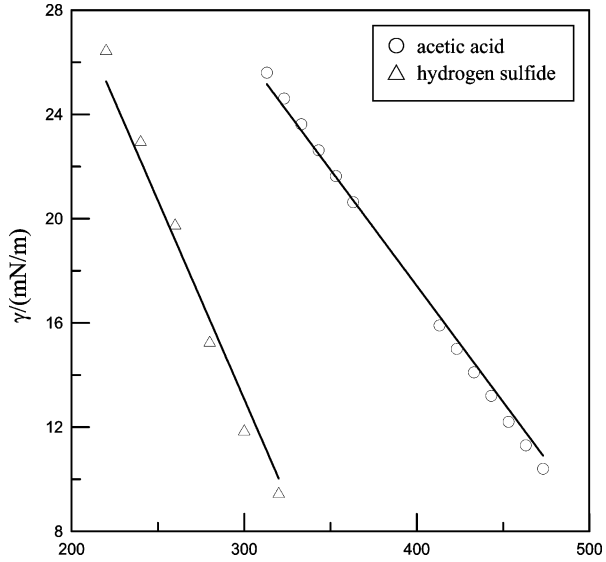

Figure 7. Surface tensions of acetic acid and hydrogen sulfide (symbols, experimental data;[52,53] lines, calculated with the MFMT).

acknowledges financial support from the North China Electric Power University.

Nomenclature

F = Helmholtz free energy, J
f = Helmholtz free energy density, J·m^{-3}
g = radial distribution function
k = Boltzmann constant, J·K^{-1}
M = number of association sites
m = number of segments in one molecule
N = number of molecules
p = pressure, Pa
$\mathbf{r}$ = segmental position
$\mathbf{R}$ = molecular configuration
T = absolute temperature, K
u = potential, J
X = mole fraction of molecules not bonded at site A
Z = compressibility factor

Greek Letters

$\beta = 1/kT$
Δ = association strength, m^3
ϵ = dispersion energy parameter, J
ϵ^{AB} = association energy parameter, J
γ = surface tension, mN·m^{-1}
κ^{AB} = association volume
Λ = de Broglie thermal wavelength, m
λ = range parameter for Yukawa potential, $\lambda = 1.8$.
λ = wavelength, m
μ = chemical potential, J·mol^{-1}
ρ = mass density, kg·m^{-3}
ρ = number density of molecules, m^{-3}
σ = hard-core diameter of a segment
Ω = grand potential

Superscripts

assoc = association
chain = chain formation
dis = dispersion
hs = hard sphere
id = ideal

Subscripts

c = critical point
L = liquid
l = long-ranged correlation
s = short-ranged correlation
V = vapor

Appendix I:

Expressions for the partial derivatives appearing in eq 27

$$\frac{\partial f^{\mathrm{id}}[\rho(z)]}{\partial \rho(z)} = kT \ln[\rho(z)\Lambda^3] \tag{I.A}$$

$$\frac{\partial f^{\mathrm{ref}}[\rho(z)]}{\partial \rho(z)} = \int_{z-R}^{z+R} \sum_{\alpha} \frac{\partial f^{\mathrm{ref}}[n_\alpha(z')]}{\partial n_\alpha(z')} W^{(\alpha)}(z,z')\, \mathrm{d}z' \tag{I.B}$$

with $\Delta z = z - z'$, $W^{(V_2)}(z,z') = 2\pi(-\Delta z)(\mathbf{z}/z')$, $W^{(3)}(z - z') = \pi[R^2 - \Delta z^2]$, $W^{(2)}(z - z') = 2\pi R$, and

$$n_\alpha(z) = \int_{z-R}^{z+R} \rho(z')\, W^{(\alpha)}(z,z')\, \mathrm{d}z'$$

$$\frac{\partial f^{\mathrm{dis}}[\rho(z)]}{\partial \rho(z)} = \frac{\partial f_0^{\mathrm{dis}}[\rho(z)]}{\partial \rho(z)} + \frac{\partial f_1^{\mathrm{dis}}[\rho(z)]}{\partial \rho(z)} \tag{I.C}$$

where $f_0^{\mathrm{dis}}[\rho(z)]$ is the attractive Helmholtz energy density of a uniform fluid with density $\rho(z)$. Accordingly, on the LDA, $\partial f_0^{\mathrm{dis}}[\rho(z)]/\partial\rho(z)$ is given by

$$\frac{\partial f_0^{\mathrm{dis}}[\rho(z)]}{\partial \rho(z)} = mF_0^{\mathrm{dis}}[\rho(z)] + mZ_0^{\mathrm{dis}}[\rho(z)] \tag{I.D}$$

where Z_0^{dis} is the compressibility factor due to the attractive contribution for uniform fluids,[42] which is expressed in Appendix II. Using the weighted densities as they appear in the MFMT, we can express $\partial f_0^{\mathrm{dis}}[\rho(z)]/\partial\rho(z)$ as

$$\frac{\partial f_0^{\mathrm{dis}}[\rho(z)]}{\partial \rho(z)} = \int_{z-R}^{z+R} \sum_{\alpha} \frac{\partial f_0^{\mathrm{dis}}[n_\alpha(z')]}{\partial n_\alpha(z')} W^{(\alpha)}(z,z')dz' \tag{I.E}$$

In our calculation, only $\alpha = 3$ is taken into account in eq I.E. We find that this is sufficient to achieve smooth but convergent density profile.

$$\frac{\partial f_1^{\mathrm{dis}}[\rho(z)]}{\partial \rho(z)} = \frac{f_1^{\mathrm{dis}}[\rho(z) + \Delta\rho(z)] - f_1^{\mathrm{dis}}[\rho(z) - \Delta\rho(z)]}{2\Delta\rho(z)} \tag{I.F}$$

$$f_1^{\mathrm{dis}}[\rho(z)] = \frac{kTm^2}{4} \int [\rho(z) - \rho(z')]^2 \overline{c(|z - z'|;\bar{\rho})}\, \mathrm{d}z' \tag{I.G}$$

where the average direct correlation function $\overline{c(|z-z'|;\bar{\rho})}$ is expressed as

$$\overline{c(|z - z'|;\bar{\rho})} = \int_0^{2\pi} \mathrm{d}\theta \int c[(\theta,r,|z - z'|);\bar{\rho}]r\, \mathrm{d}r \tag{I.H}$$

Appendix II: Expressions for f_0^{dis} and Z_0^{dis}

The following definitions are used to calculate the Helmholtz free energy density, f_0^{dis}, for pure fluids with the Yukawa potential

$$f_0^{\mathrm{dis}} = \rho F_0^{\mathrm{dis}} \tag{II.A}$$

$$\frac{F_0^{\text{dis}}}{NkT} = -\frac{\alpha_0}{\phi_0}\beta\epsilon - \frac{\lambda^3}{6\eta}\left[F(x) - F(y) - (x-y)\frac{\mathrm{d}F(y)}{\mathrm{d}y}\right] \quad \text{(II.B)}$$

$$Z_0^{\text{dis}} = -\eta\frac{\beta\epsilon}{\phi_0}\left(\frac{\partial\alpha_0}{\partial\eta} - \frac{\alpha_0}{\phi_0}\frac{\partial\phi_0}{\partial\eta}\right) + \frac{\lambda^3}{6\eta}\left[F(x) - F(y) - (x-y)\frac{\mathrm{d}F(y)}{\mathrm{d}y}\right] - \frac{\lambda^3}{6}\left\{\frac{\partial x}{\partial\eta}\left[\frac{\mathrm{d}F(x)}{\mathrm{d}x} - \frac{\mathrm{d}F(y)}{\mathrm{d}y}\right] - \frac{\partial y}{\partial\eta}(x-y)\frac{\mathrm{d}^2F(y)}{\mathrm{d}y^2}\right\} \quad \text{(II.C)}$$

where $\lambda = 1.8$ is the range parameter for hard-core Yukawa fluids, $\beta = 1/kT$, $\eta = \pi\rho\sigma^3/6$, and

$$x = \frac{(1+\lambda\psi)w}{\lambda^2}\beta\epsilon, \qquad y = \frac{w\psi}{\lambda}\beta\epsilon, \qquad w = 6\eta/{\phi_0}^2 \quad \text{(II.D)}$$

$$\psi = \frac{\lambda^2(1-\eta)^2(1-\mathrm{e}^{-\lambda}) - 12\eta(1-\eta)[1-\lambda/2-(1+\lambda/2)\mathrm{e}^{-\lambda}]}{\mathrm{e}^{-\lambda}L(\lambda) + S(\lambda)} \quad \text{(II.E)}$$

$$\alpha_0 = \frac{L(\lambda)}{\lambda^2(1-\eta)^2}, \qquad \phi_0 = \frac{\exp(-\lambda)L(\lambda) + S(\lambda)}{\lambda^3(1-\eta)^2} \quad \text{(II.F)}$$

$$F(x) = -\frac{1}{4}\ln(1-2x) - 2\ln(1-x) - \frac{3}{2}x - \frac{1}{1-x} + 1 \quad \text{(II.G)}$$

$$L(\lambda) = 12\eta[(1+\eta/2)\lambda + 1 + 2\eta] \quad \text{(II.H)}$$

$$S(\lambda) = (1-\eta)^2\lambda^3 + 6\eta(1-\eta)\lambda^2 + 18\eta^2\lambda - 12\eta(1+2\eta) \quad \text{(II.I)}$$

Literature Cited

(1) Krantz, W. B., Wasan, D. T., Jain, R. K., Eds. *Thin Liquid Film Phenomena*; American Institute of Chemical Engineers: New York, 1986.

(2) Wasan, D. T.; Payatakes, A. *Interfacial Phenomena in Enhanced Oil Recovery*; American Institute of Chemical Engineers: New York, 1982.

(3) Wasan, D. T.; Ginn, M. E.; Shah, D. O. *Surfactants in Chemical/Process Engineering*; Marcel Dekker: New York, 1988.

(4) Edwards, D. A.; Brenner, H., Wasan, D. T. *Interfacial Transport Processes and Rheology*; Butterworth-Heinemann: Boston, 1991.

(5) Adamson, A. W.; Gast, A. P. *Physical Chemistry of Surfaces*; Wiley: New York, 1997.

(6) Hiemenz, P. C.; Rajagopalan, R. *Principles of Colloid and Surface Chemistry*; Marcel Dekker: New York, 1997.

(7) Nicholson, D.; Parsonage, N. G. *Computer Simulation and the Statistical Mechanics of Adsorption*; Academic Press: London1982.

(8) Davis, H. T. *Statistical Mechanics of Phases, Interfaces, and Thin Films*; VCH: New York, 1996.

(9) Hohenberg, P.; Kohn, W. *Phys. Rev.* **1964**, *136*, B864.

(10) Evans, R. Density functionals in the theory of nonuniform fluids. In *Fundamentals of Inhomogeneous Fluids*; Henderson, D., Ed.; Marcel Dekker: New York, 1992; p 85.

(11) Lowen, H. Density functional theory: From statics to dynamics. *J. Phys.: Condens. Matter* **2003**, *15*, V1.

(12) Oxtoby, D. W. Density functional methods in the statistical mechanics of materials. *Annu. Rev. Mater. Res.* **2002**, *32*, 39.

(13) Yu, Y. X.; Wu, J. Z. A fundamental-measure theory for inhomogeneous associating fluids. *J. Chem. Phys.* **2002**, *116*, 7094.

(14) Yu, Y. X.; Wu, J. Z. Structures of hard sphere fluids from a modified fundamental measure theory. *J. Chem. Phys.* **2002**, *117*, 10156.

(15) Yu, Y. X.; Wu, J. Z. Density functional theory for inhomogeneous mixtures of polymeric fluids. *J. Chem. Phys.* **2002**, *117*, 2368.

(16) Yu, Y. X.; Wu, J. Z. A Modified Fundamental Measure Theory for Spherical Particles in Microchannels. *J. Chem. Phys.* **2003**, *119*, 2288.

(17) Yu, Y. X.; Wu, J. Z.; Gao, G. H. Density Functional Theory for Spherical Electrical Double Layers and Zeta Potentials of Colloidal Particles in Restricted-Primitive-Model Electrolyte Solutions. *J. Chem. Phys.* **2004**, *120*, 7223.

(18) Yu, Y.-X.; Wu, J. Extended test-particle method for predicting the inter- and intramolecular correlation functions of polymeric fluids. *J. Chem. Phys.* **2002**, *118*, 3835.

(19) Tang, Y. P.; Wu, J. Z. A new density functional theory of uniform and inhomogeneous Lennard-Jones fluids from the energy route. *J. Chem. Phys.* **2003**, *109*, 7388.

(20) Tang, Y. P.; Wu, J. Z. Modeling Inhomogeneous van der Waals Systems Using an Analytical Direct Correlation Function. *Phys. Rev. E* **2004**, *70*, 018407.

(21) Li, Z. D.; Wu, J. Z. Microstructures and Thermodynamic Properties of Colloidal Dispersions Mimicking Macromolecular Crowding. *Phys. Rev. E*, manuscript accepted.

(22) Chapman, W. G.; Jackson, G.; Gubbins, K. E. Phase equilibria of associating fluids: Chain molecules with multiple bonding sites. *Mol. Phys.* **1988**, *65*, 1057.

(23) Chapman, W. G.; Gubbins, K. E.; Jackson, G.; Radosz, M. SAFT: Equation-of-State Solution Model for Associating Fluids. *Fluid Phase Equilib.* **1989**, *52*, 31.

(24) Segura, C. J.; Chapman, W. G. Shukla, K. P. Associating fluids with four bonding sites against a hard wall: density functional theory. *Mol. Phys.* **1997**, *90*, 759.

(25) Segura, C. J.; Vakarin, E. V.; Chapman, W. G.; Holovko, M. F. A comparison of density functional and integral equation theories vs Monte Carlo simulations for hard sphere associating fluids near a hard wall. *J. Chem. Phys.* **1998**, *108*, 4837.

(26) Tripathi, S.; Chapman, W. G. Density-functional theory for polar fluids at functionalized surfaces. I. Fluid-wall association. *J. Chem. Phys.* **2003**, *119*, 12611.

(27) Tripathi, S.; Chapman, W. G. A density functional approach to chemical reaction equilibria in confined systems: Application to dimerization. *J. Chem. Phys.* **2003**, *118*, 7993.

(28) Pizio, O.; Reszko-Zygmunt, J.; Patrykiejew, A. Sokolowski, S. Microscopic structure and properties of an interface between coexisting phases of an associating fluid adsorbed in slitlike pores. *J. Colloid Interface Sci.* **2003**, *260*, 126.

(29) Alejandre, J.; Duda, Y. Sokolowski, S. Computer modeling of the liquid−vapor interface of an associating Lennard-Jones fluid. *J. Chem. Phys.* **2003**, *118*, 329.

(30) Malo, B. M.; Pizio, O.; Patrykiejew, A.; Sokolowski, S. Adsorption and phase transitions in a two-site associating Lennard-Jones fluid confined to energetically heterogeneous slit-like pores: Application of the density functional method. *J. Phys.: Condens. Matter* **2001**, *13*, 1361.

(31) Pizio, O.; Patrykiejew, A.; Sokolowski, S. Evaluation of liquid−vapor density profiles for associating fluids in pores from density-functional theory. *J. Chem. Phys.* **2000**, *113*, 10761.

(32) Huerta, A.; Pizio, O.; Bryk, P.; Sokolowski, S. Application of the density functional method to study phase transitions in an associating Lennard-Jones fluid adsorbed in energetically heterogeneous slit-like pores. *Mol. Phys.* **2000**, *98*, 1859.

(33) Malo, B. M.; Bryk, P.; Duda, Y.; Pizio, O. Application of the density functional method to study adsorption and phase transitions in two-site associating, Lennard-Jones fluids in cylindrical pores. *J. Phys.: Condens. Matter* **2000**, *12*, 8785.

(34) Patrykiejew, A.; Salamacha, L.; Sokolowski, S.; Pizio, O. Wetting behavior of associating binary mixtures at attractive walls: A lattice Monte Carlo study. *Phys. Rev. E*, **2003**, *67*.

(35) Bucior, K.; Patrykiejew, A.; Sokolowski, S.; Pizio, O. Liquid−liquid interface in a binary mixture of associating fluids exhibiting a closed-loop immiscibility. *Mol. Phys.* **2003**, *101*, 2233.

(36) Talanquer, V.; Oxtoby, D. W. Gas−liquid nucleation in associating fluids. *J. Chem. Phys.* **2000**, *112*, 851.

(37) Talanquer, V.; Oxtoby, D. W. A density-functional approach to nucleation in micellar solutions. *J. Chem. Phys.* **2000**, *113*, 7013.

(38) Fu, D.; Wu, J. A self-consistent approach for modeling the interfacial properties and phase diagrams of Yukawa, Lennard-Jones and square-well fluids, *Mol. Phys.*, manuscript submitted.

(39) Roth, R.; Evans, R.; Lang, A.; Kahl, G. Fundamental measure theory for hard-sphere mixtures revisited: The White Bear Version. *J. Phys.: Condens. Matter* **2002**, *14*, 12063.

(40) Rosenfeld, Y. Free-energy model for the inhomogeneous hard-sphere fluid mixture and density-functional theory of freezing. *Phys. Rev. Lett.* **1989**, *63*, 980.

(41) Carnahan, N. F.; Starling, K. E. Equation of state for nonattracting rigid spheres. *J. Chem. Phys.* **1969**, *51*, 635.

(42) Duh, D. M.; MierYteran, L. An analytical equation of state for the hard-core Yukawa fluid. *Mol. Phys.* **1997**, *90*, 373.

(43) Tang, Y. P.; Lu, B. C. Y. On the mean spherical approximation for the Lennard-Jones fluid. *Fluid Phase Equilib.* **2001**, *190*, 149.

(44) Tang, Y. P. On the first-order mean spherical approximation. *J. Chem. Phys.* **2003**, *118*, 4140.

(45) Ebner, C.; Saam, W. F.; Stroud, D. Density-functional theory of simple classical fluids. I. Surfaces. *Phys. Rev. A: Gen. Phys.* **1976**, *14*, 2264.

(46) White, J. A.; Zhang, S. Renormalization Group Theory for Fluids. *J. Chem. Phys.* **1993**, *99*, 2012.

(47) White, J. A.; Zhang, S. Renormalization Theory of Nonuniversal Thermal Properties of Fluids. *J. Chem. Phys.* **1995**, *103*, 1922.

(48) Lue, L.; Prausnitz, J. M. Renormalization-group corrections to an approximate free-energy model for simple fluids near to and far from the critical region. *J. Chem. Phys.* **1998**, *108*, 5529.

(49) Jiang, J. W.; Prausnitz, J. M. Equation of state for thermodynamic properties of chain fluids near-to and far-from the vapor-liquid critical region. *J. Chem. Phys.* **1999**, *111*, 5964.

(50) Tang, Y. P. Outside and inside the critical region of the Lennard-Jones fluid. *J. Chem. Phys.* **1998**, *109*, 5935.

(51) Fu, D.; Li, Y. G.; Wu, J. Effect of the range of attractive interactions on crystallization, metastable phase transition and percolation in colloidal disperions. *Phys. Rev. E* **2003**, *68*, 011403.

(52) Beaton, C. F.; Hewitt, G. F. *Physical Property Data for the Design Engineer*; Hemisphere Publishing Corp.: New York, 1989.

(53) Jasper, J. J. The surface tension of pure liquid compounds. *J. Phys. Chem. Ref. Data* **1972**, *1*, 841.

Received for review March 18, 2004
Revised manuscript received May 25, 2004
Accepted May 31, 2004

IE049788A